THE JOURNAL OF BIOLOGICAL CHEMISTRY
Vol. 274, No. 5, Issue of January 29, pp. 2988–3000, 1999

Printed in U.S.A.

Pyropheophorbide-a Methyl Ester-mediated Photosensitization Activates Transcription Factor NF-κB through the Interleukin-1 Receptor-dependent Signaling Pathway*

(Received for publication, July 1, 1998, and in revised form, November 4, 1998)

Jean-Yves Matroule‡§, Giuzeppina Bonizzi¶‖, Patrice Morlière, Nicole Paillous‡‡, René Santus**, Vincent Bours¶§§, and Jacques Piette‡¶¶**

*From the ‡Laboratory of Virology, ¶Laboratory of Medical Chemistry, Institute of Pathology B23, University of Liège, B-4000 Liège, Belgium, the **Muséum National d'Histoire Naturelle, F-75231 Paris Cedex 05, and ‡‡IMRCP Laboratory, CNRS-URA 470, University of Toulouse, F-31062 Toulouse, France*

Pyropheophorbide-a methyl ester (PPME) is a second generation of photosensitizers used in photodynamic therapy. We demonstrated that PPME photosensitization activated NF-κB transcription factor in colon cancer cells. Unexpectedly, this activation occurred in two separate waves, *i.e.* a rapid and transient one and a second slower but sustained phase. The former was due to photosensitization by PPME localized in the cytoplasmic membrane which triggered interleukin-1 receptor internalization and the transduction pathways controlled by the interleukin-1 type I receptor. Indeed, TRAF6 dominant negative mutant abolished NF-κB activation by PPME photosensitization, and TRAF2 dominant negative mutant was without any effect, and overexpression of IκB kinases increased gene transcription controlled by NF-κB. Oxidative stress was not likely involved in the activation. On the other hand, the slower and sustained wave could be the product of the release of ceramide through activation of the acidic sphingomyelinase. PPME localization within the lysosomal membrane could explain why ceramide acted as second messenger in NF-κB activation by PPME photosensitization. These data will allow a better understanding of the molecular basis of tumor eradication by photodynamic therapy, in particular the importance of the host cell response in the treatment.

Photodynamic therapy (PDT)[1] is a new cancer treatment modality that selectively destroys malignant, premalignant, and benign lesions in patients (1–3) and is initiated by the selective accumulation of a photosensitizing agent in malignant tissue. The sensitizer is harmless unless and until activated by light of the appropriate wavelength. This results in a photochemical reaction leading to tumor destruction through a combination of direct photodamage to cancer cells as well as tumor stroma, especially the microvasculature of the tumor bed and the surrounding tissues (4). The majority of photodynamic agents is provided exogenously via intravenous injection with subsequent uptake of the drug by tissues. The only drug currently approved for therapy is a porphyrin oligomer (Photofrin) which is highly effective but exhibits several drawbacks such as (i) a tendency to cause prolonged skin photosensitivity; (ii) an activation wavelength lower than that optimal for effective penetration through tissue; and (iii) a poorly defined chemical composition that makes a detailed understanding of its mode of action and pharmacokinetics difficult. To address these issues, new photosensitizers are being developed, and a number of new agents are now in clinical trials. Several groups have recently reported the antitumor efficacy of pheophorbide- and pyropheophorbide-based photodynamic therapy (5–7). These compounds are chemically well characterized, absorb light above 600 nm, and produce less long term normal tissue phototoxicity than Photofrin. In the pyropheophorbide-a series, either as methyl esters or as carboxylic acids, photosensitizing efficacy increases with the length of the alkyl ether side chain, but the alkyl ether derivatives, although having similar photophysical properties (singlet oxygen and fluorescence yields), exhibit remarkable differences in photosensitizing efficiency (8). These results suggest that besides hydrophobicity, steric factors and conformation of the alkyl side chains influence localization in the cells.

There are several lines of evidence suggesting that singlet oxygen ($^1O_2$) is the major damaging species in PDT (9–12). Other reactive oxygen species (ROS) may also be involved in the biological effects caused by PDT (13), particularly in the case of porphyrin derivatives used as photosensitizers (8, 14). Photochemically targeted $^1O_2$ is mainly responsible for cytotoxicity caused by PDT. If target cells are not destroyed, photooxidative stress may modulate the activation of nuclear transcription factors that regulate the expression of stress response genes. The cellular redox state is known to be involved in regulation of gene expression, and ROS may act as chemical messengers modulating gene expression via the activation of transduction pathways (15, 16). Currently, the biological effects resulting from PDT-induced changes in gene expression and signal transduction are largely unknown. As a further step toward understanding modulation of gene expression by PDT, we report here the mechanism of NF-κB activation in colon cancer cells by pyropheophorbide-a methyl ester (PPME), a

* This work was supported in part by grants from the Belgian National Fund for Scientific Research (NFSR, Brussels, Belgium), from the Concerted Action Program (University of Liège), and from Télévie (NFSR, Brussels, Belgium). The costs of publication of this article were defrayed in part by the payment of page charges. This article must therefore be hereby marked "*advertisement*" in accordance with 18 U.S.C. Section 1734 solely to indicate this fact.

§ Research fellow from the Fonds de Recherche Industrielle et Agricole (Brussels, Belgium).

‖ Supported by the European Community (Biotech Program).

§§ Research associate from the Belgian National Fund for Scientific Research.

¶¶ Research director from the Belgian National Fund for Scientific Research. To whom correspondence should be addressed: Laboratory of Virology, Institute of Pathology B23, University of Liège, B-4000 Liège, Belgium. Tel.: 32-4-366.24.42; Fax: 32-4-366.24.33; E-mail: jpiette@ulg.ac.be.

[1] The abbreviations used are: PDT, photodynamic therapy; PPME, pyropheophorbide-a methyl ester; $^1O_2$, singlet oxygen; ROS, reactive oxygen species; IL, interleukin; TNF-α, tumor necrosis factor α; IKK, IκB kinase; SMase, sphingomyelinase, FCS, fetal calf serum; DiOC6, 3,3′-dihexylpxacarbocyanine iodide; EMSA, electrophoretic mobility shift assay.

second generation photosensitizer showing great promise in PDT. Since cytokine release during PDT may have important biological effects for surrounding cells, we decided to focus our attention on transcription factor NF-κB because it is a redox-activated transcription factor involved in the control of genes encoding several important cytokines such as interleukin (IL)-1, IL-2, and IL-6 and tumor necrosis factor (TNF)-α as well as chemokines such as IL-8, regulated on activation normal T cell expressed and secreted, and macrophage inflammatory protein-1 (see Ref. 17 for review).

NF-κB complexes bind DNA as dimers constituted from a family of proteins designated as the Rel/NF-κB family. In mammals, this family contains proteins p50, p52, p65 (RelA), RelB, and c-Rel (Rel) (18, 19). These five proteins harbor a related, but non-identical 300-amino acid long Rel homology domain that is responsible for dimerization, nuclear translocation, and specific DNA-binding. In addition, RelA, RelB, and c-Rel, but not p50 or p52, contain one or two transactivating domains. p50 and p52 derive from cytoplasmic precursors named p105 and p100, respectively. NF-κB complexes are sequestered in the cytoplasm of most resting cells by inhibitory proteins belonging to the IκB family (20–23). The members of the IκB family are IκBα, IκBβ, IκBϵ, p100, and p105.

Following various stimuli, including the interaction of TNF-α and IL-1β with their receptors, IκBα is first phosphorylated on serines 32 and 36, then ubiquitinated at lysines 21 and 22, and rapidly degraded by the proteasome, allowing NF-κB nuclear translocation and gene activation (24, 25). In the case of these two types of cytokines, the signal transduction pathways leading to the phosphorylation and degradation of IκB proteins have recently been clarified in HeLa and L293 cells (26–30). It is included in a 700–900-kDa complex called signalosome whose important partners are proteins associated to the TNF-α or IL-1 receptors, NF-κB-inducing kinase, IKK-α, -β, and -γ (26–31). Pro-inflammatory cytokines such as TNF-α or IL-1β or the bacterial outer membrane component (lipopolysaccharide) are potent activators of NF-κB, which mediate several of their biological activities such as stimulation of the transcription in lymphocytes through the intracellular generation of oxidative stress (32, 33). However, the assumption that a similar mechanism is effective in other cell lines has not yet been demonstrated.

In this paper, we report that PPME-mediated PDT of colon cancer cells activates NF-κB, by triggering the signaling pathway controlled by the IL-1 receptor likely without involvement of ROS. By increasing IL-1 receptor internalization, PPME photosensitization also leads to the activation of the acidic sphingomyelinase (SMase) with intracellular release of ceramide. Furthermore, our data suggest that, as a consequence of PPME-mediated PDT, surviving colon cancer cells could influence surrounding cells by releasing factors whose encoding genes are controlled by NF-κB.

MATERIALS AND METHODS

Chemicals and Reagents—Pyropheophorbide methyl ester (PPME) was from Sigma and was used without any further purification. A stock solution was made in ethanol (1 mM) and kept in the dark at −20 °C. PPME was diluted in the culture medium just before use and added to exponentially growing cells. The fluorescent probes used for cellular localization studies were purchased from Molecular Probes-Europe (Leiden, The Netherlands). Radiolabeled nucleotides were from ICN (United Kingdom), and ^{125}I-labeled IL-1β and TNF-α were from NEN Life Science Products (United Kingdom) or Amersham Pharmacia Biotech (United Kingdom). Deuterium oxide was 99.8% pure from Merck (Germany). All other chemicals were of reagent grade. Anti-IκBα monoclonal antibody was obtained from C. Dargemont (Curie Institute, Paris); anti-IκBβ was obtained from Santa Cruz Biotechnology; anti-p100 monoclonal and anti-p105 polyclonal antibodies were obtained from U. Siebelnist (National Institutes of Health, Bethesda).

Cell Culture—The human colon carcinoma cell line HCT-116 was grown in McCoy's 5A medium (Life Technologies, Inc., United Kingdom) supplemented with 10% fetal calf serum (FCS, Life Technologies, Inc.). Before photosensitization with PPME, HCT-116 cells were grown for 1 week in 2% FCS. HCT-116 cells overexpressing IκBα mutated either at serines 32 and 36 (S32A, S36A) or at tyrosine 42 (Y42F) were obtained after transfection with the corresponding expression plasmids bearing a gene conferring resistance to neomycin. After a classical selection procedure (500 μg/ml neomycin), cells were cloned and expanded in the presence of neomycin (250 μg/ml).

Plasmids—pNF-κB-Luc reporter construct contains 5 κB sites from the human immunodeficiency virus type-1 long terminal repeat cloned upstream of the luciferase gene (Stratagene). pTRAF6, pΔ TRAF6-(289–522) (34), pΔ TRAF2-(87–501) (35), and pIKK-α or -β constructs were gifts from D. Goeddel (Tularik). pIκBα S32A,S36A was obtained from A. Israel (Pasteur Institute, France) and pIκBαY42F was obtained from J-F. Peyron (Nice, France). All plasmids were purified using Qiagen column chromatography (Qiagen, The Netherlands), and integrity was checked by agarose gel electrophoresis.

Exposure of HCT-116 Cells to PPME Photosensitization—Before photosensitization with PPME, HCT-116 cells were cultivated for 1 week in McCoys 5A medium with 2% FCS and incubated with 2 μM PPME during the last 20 h. Prior to irradiation, HCT-116 cells were washed twice with PBS and then irradiated with red light (λ >600 nm) at a fluence rate of 160 watts/m^2 in Petri dishes covered with PBS. After irradiation, HCT-116 cells were put back in culture at 37 °C in McCoys 5A medium supplemented with 2% FCS. Cell survival was determined after 24 h using trypan blue exclusion. Photosensitization with PPME was carried out to attain 50% cell survival after 24 h.

Cellular Localization and Microspectrofluorimetry—Co-localization experiments and intracellular fluorescence spectroscopy were carried out with a proprietary microspectrofluorometer constructed around a Leitz "Diavert" inverted microscope equipped with a heated stage which was maintained at 37 ± 1 °C (36, 37). Fluorescence excitation was performed over the whole microscope field with 405 nm light from a 100-watt super-high pressure mercury lamp (~1 watt/cm^2 without neutral filter). A bidimensional adjustable slit in the primary image plane limited the area in the microscopic field from which the fluorescence could be collected through a selected filter. In the topographic mode, fluorescence light was reflected by a mirror to the bidimensional cooled CCD target (1024 × 1024 pixels), which was coupled to signal recording and processing software (Photometrics, Tucson, AZ). Images of 400 × 400 superpixels (2 × 2 binning) corresponding to a 46 × 46-μm field were recorded, and the exposure time was equal to 4 s. In the spectrotopographic mode, 150 grooves/nm grating replaced the mirror. The slit was reduced to a narrow strip and used as the entrance to the grating, delineating in the object plane a 2-μm-wide strip along the whole field from which fluorescence was collected. This slit provided a spectral resolution of about 5 nm. Fluorescence photons received by the bidimensional detector produced a spectrotopographic image. Such images (335 × 335 superpixels) recorded with a 2 × 2 binning can be interpreted as either a succession, in the *x* direction, of linear monochromatic images of a 2-μm-wide strip or a succession of spectra along the *y* axis (46 μm), each corresponding to an area of 2 × 0.15 μm^2 of the strip. Exponentially growing HCT 116 cells were grown as monolayers in custom-made glass-bottom chambers designed for use with this microspectrofluorometer.

Electrophoretic Mobility Shift Assay (EMSA)—Nuclear extracts were isolated as described by a rapid micropreparation technique derived from the large scale procedure of Dignam *et al.* (38) based on the use of a lysis with detergent (Nonidet P-40) followed by high salt extraction of nuclei (39). Binding reactions were performed for 25 min at room temperature with 7.5 μg of total protein in 20 μl of 20 mM HEPES-KOH, pH 7.9, 75 mM NaCl, 1 mM EDTA, 5% glycerol, 0.5 mM $MgCl_2$, 2 μg of acetylated bovine serum albumin, 4 μg of poly(dI-dC)·poly(dI-dC) (Amersham Pharmacia Biotech, U. K.), 1 mM dithiothreitol, and 0.2 ng of ^{32}P-labeled oligonucleotides (Eurogentech, Belgium). Oligonucleotides were labeled by end-filling with the Klenow fragment of *Escherichia coli* DNA polymerase I (Boehringer Mannheim, Germany) with [^{32}P]dATP, [^{32}P]dCTP (NEN Life Science Products or ICN, United Kingdom), and cold dTTP + dGTP. Labeled probes were purified by spin chromatography on G-25 columns. DNA-protein complexes were separated from unbound probe on native 6% polyacrylamide gels at 150 V in 0.25 M Tris, 0.25 M sodium borate, and 0.5 mM EDTA, pH 8.0. Gels were vacuum-dried and exposed to Fuji x-ray film at −80 °C for 16–24 h. The amounts of specific complexes were determined either by counting the radioactivity with a PhosphorImager (Molecular Dynamics) or by photodensitometry (LKB, Sweden) of the autoradiography. Supershift ex-

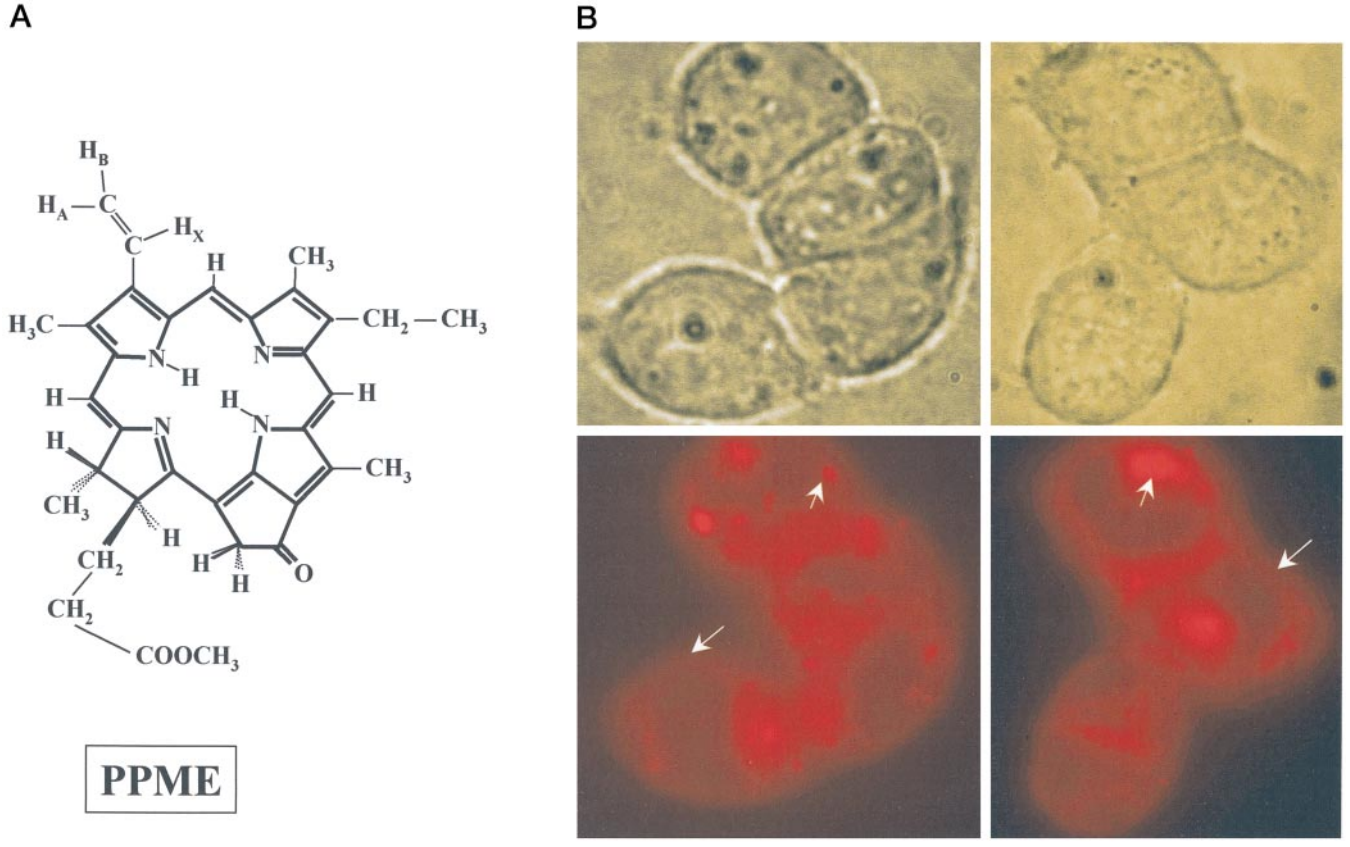

FIG. 1. *A,* chemical structure of PPME. *B,* localization of PPME in HCT-116 cells. Cells were mixed with 2 μM PPME in the dark and mounted on slides before being observed by fluorescence microscopy (λ_{exc} = 515–560 nm) and under phase contrast microscopy. *Arrows* indicated PPME localization at the cytoplasmic membranes or in several internal compartments.

periments were carried out as described (40), using the same EMSA protocol as described above except for the gel concentration being 4%. The sequences of the probes (Eurogentech, Belgium) used in this work are as shown in Sequence 1.

```
Wild-type NF-κB probe      5′-GGTTACAAGGGACTTTCCGCTG
                                TGTTCCCTGAAAGGCGACGGTT-5′

Mutated NF-κB probe      5′-GGTTAACAACTCACTTTCCGCTG
                              TTGTTGAGTGAAAGGCGACGGTT-5′
```

SEQUENCE 1

IκBα, IκBβ, p105, and p100 Detection—IκBα, IκBβ, p105, and p100 inhibitory subunits were detected by Western blot analysis using specific antibodies. Cytoplasmic extracts were prepared at various times after the photosensitization by cell lysis with a detergent (Nonidet P-40), pelleting the nuclei, and collecting the supernatant fraction (41). Cytoplasmic proteins were added to a loading buffer (10 mM Tris-HCl, pH 6.8, 1% SDS, 25% glycerol, 0.1 mM β-mercaptoethanol, 0.03% bromphenol blue), boiled, and electrophoresed on a 12% polyacrylamide-SDS gel and electro-transferred to Immobilon-P membranes (Millipore, United Kingdom). Filters were incubated with anti-IκBα (1:500 dilution), anti-IκBβ (1:500 dilution), anti-p105 (1:1700 dilution), or anti-p100 (1:2000 dilution) antibodies for 60 min at room temperature, then with peroxidase-conjugated goat anti-rabbit IgG or anti-mouse IgG (1:500 dilution) for 60 min at room temperature, and finally analyzed using Amersham's enhanced chemiluminescence system (ECL) (Amersham Pharmacia Biotech, United Kingdom) with Fuji x-ray film.

Cytokine Receptor Internalization—Cytokine receptor internalization was carried out as described (42). In short, HCT-116 cells were first washed in PBS, trypsinized, and counted. The cell pellet was resuspended in 100 μl of binding buffer (McCoy's 5A-10% FCS plus 0.2% bovine serum albumin) and 1 μl of ^{125}I-labeled cytokine (20,000 Bq/assay) and incubated for 2 h at 4 °C with shaking before being placed at 37 °C to initiate internalization. Cells were then centrifuged at 14,000 × *g* for 30 s, and the pellet was resuspended in 100 μl of acidic buffer (50 mM glycine, pH 3.0) and placed on ice for 90 s. Binding buffer (600 μl) was then added to the cells, centrifuged at 14,000 × *g* for 30 s, and the supernatant recovered and counted. The pellet was resuspended in 70 μl of binding buffer and loaded on 300 μl of 20% (w/v) sucrose, 1% (w/v) bovine serum albumin. After centrifugation for 5 min at 14,000 × *g*, the pellet was recovered and counted. Internalization was evaluated by determining the ratio between the radioactivity measured in the cell pellet *versus* the total radioactivity (outside + inside cells).

Transient Transfection Assays—HCT-116 cells were grown in 6-well plates for 2 days in McCoy's 5A medium supplemented with 10% FCS and transfected with 0.1 μg of κB-Luc reporter plasmid and various amounts of expression plasmids. The total concentration of plasmid was kept at 1 μg with pRC-CMV. Plasmids were mixed in Opti-MEM (Life Technologies, Inc., United Kingdom), added to Fugene liposomes (2 μl) (Boehringer Mannheim, Germany) for 15 min at room temperature, and loaded on cells in 2 ml of McCoy's 5A containing 10% FCS for 24 h. Then HCT-116 were treated either with TNF-α or IL-1β for 24 h or with PPME (2 μM) for 6 h and irradiated with red light (120 s). After irradiation, cells were cultivated for 15 h and then washed twice in PBS, lysed for 15 min, and centrifuged at 15,000 × *g* for 4 min. Luciferase activities corrected for protein amounts (Bio-Rad protein assay) were measured in supernatants.

Ceramide Generation—For total ceramide quantification, HCT-116 cells were incubated before treatment for 24 h in McCoy's 5A medium with 2% FCS and 2 μCi/ml of 9,10-[^{3}H]palmitic acid (ICN, United Kingdom). After lipid extraction (43) and mild alkaline hydrolysis, the lower phase of the Folch extract containing the labeled sphingolipids was evaporated. Lipids were dissolved in chloroform/methanol (2:1, v/v), spotted, and separated on an analytical TLC. Ceramide was visualized by I_2 staining, and the corresponding spots were scraped and quantified by liquid scintillation counting.

Quantification of Acidic and Neutral Sphingomyelinase Activities—Sphingomyelinase (SMase) assays were performed as described previously (44, 45). HCT-116 cells were treated with or without 150 units/ml TNF-α or with 2 μM PPME and light and then incubated for various times. To measure acidic SMase activity, 50 μg of proteins were incubated for 2 h at 37 °C in a buffer containing 250 mM sodium acetate, pH 5.0, 1 mM EDTA, and 0.2 mCi/ml [*choline-methyl*-^{14}C]sphingomyelin

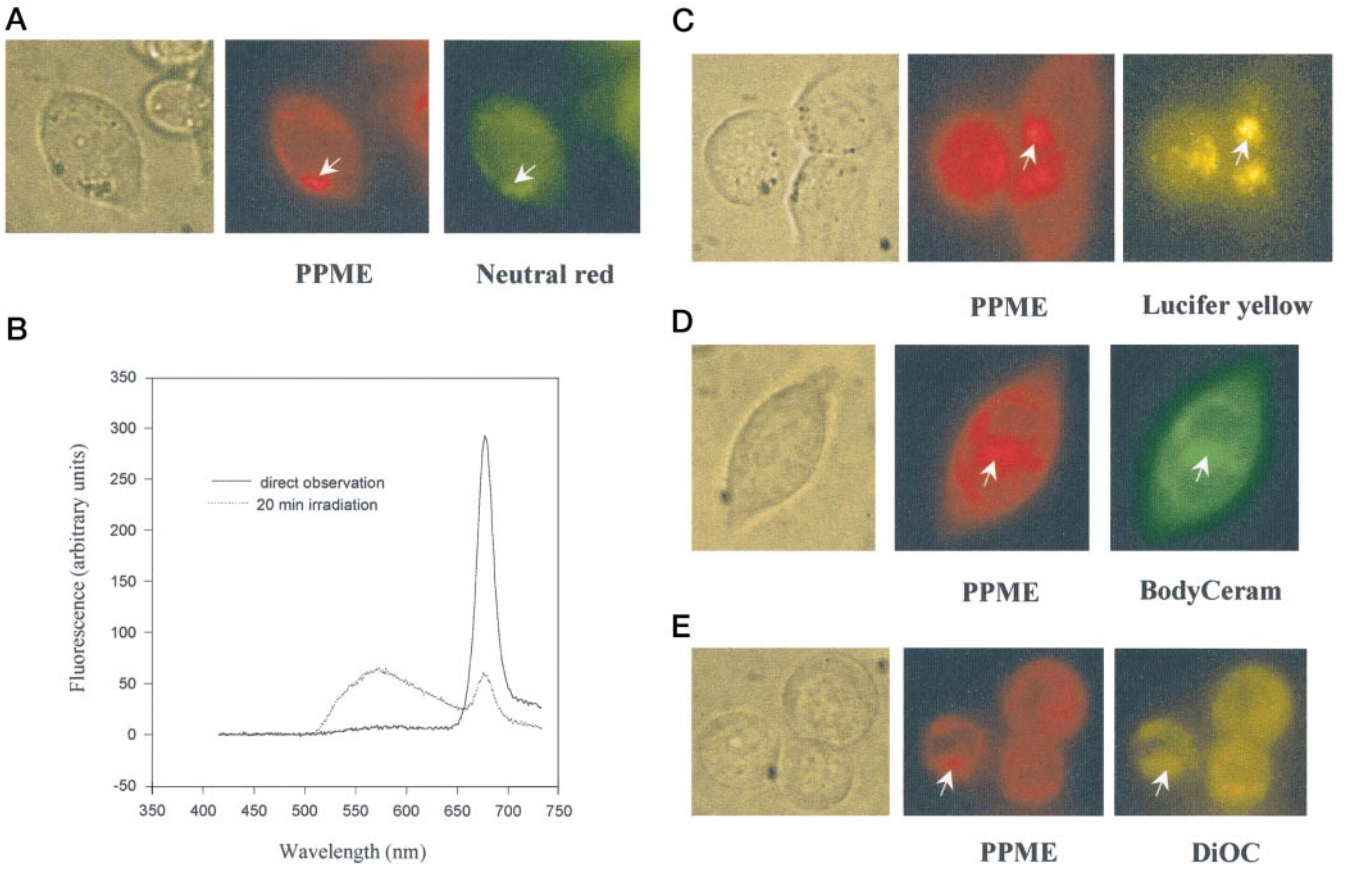

FIG. 2. *A,* cells were incubated with 1 μM PPME for 18 h and 2 μM neutral red for the last 30 min before measurements. After incubation, cells were washed twice with culture medium and left in culture medium without serum and without phenol red for measurements. *Left panel,* phase contrast image; *middle panel,* fluorescence image recorded through a 645-nm cut-off filter. Maximum intensity was about 4500 counts. *Right panel,* fluorescence recorded through a broad interference filter (540 ± 45 nm). Maximum intensity was about 150 counts. Fluorescence excitation wavelength was 405 nm. *B,* fluorescence spectra obtained from spectrotopographic images. Cells were incubated with 1 μM PPME for 18 h and 2 μM neutral red for the last 60 min. After incubation, cells were washed twice with culture medium and left in culture medium without serum and without phenol red for measurements. Spectra were averaged from three adjacent pixels. Spectra were obtained from spectrotopographic images recorded at the onset of the irradiation (*full line*) and 20 s later (*dashed line*). The fluorescence excitation and irradiation wavelength was 405 nm. *C,* cells were incubated for 18 h with 0.25 μM PPME and 1 μM lucifer yellow. After incubation, cells were washed twice with culture medium and left in culture medium without serum and without phenol red for measurements. *Left panel,* phase contrast image; *middle panel,* fluorescence image recorded through a 645-nm cut-off filter. Maximum intensity was about 600 counts. *Right panel,* fluorescence recorded through a broad interference filter (540 ± 45 nm). Maximum intensity was about 1000 counts. Fluorescence excitation wavelength was 405 nm. *D,* cells were incubated for 18 h with 0.25 μM PPME and 4 μM BodipyCeram. After incubation, cells were washed twice with culture medium and left in culture medium without serum and without phenol red for measurements. *Left panel,* phase contrast image; *middle panel,* fluorescence image recorded through a 645-nm cut-off filter. Maximum intensity was about 954 counts. *Right panel,* fluorescence recorded through a broad filter (536 nm). Maximum intensity was about 240 counts. Fluorescence excitation wavelength was 404 nm. *E,* cells were incubated for 18 h with 0.25 μM PPME and carbocyanine (DiOC, 2 mg/ml). After incubation, cells were washed twice with culture medium and left in culture medium without serum and without phenol red for measurements. *Left panel,* phase contrast image; *middle panel,:* fluorescence image recorded through a 645-nm cut-off filter. Maximum intensity was about 1252 counts. *Right panel,* fluorescence recorded through a broad filter (536 nm). Maximum intensity was about 6567 counts. Fluorescence excitation wavelength was 404 nm.

(ICN, United Kingdom; 20,000 Bq per assay). To measure neutral SMase activity, 100 μg of proteins were incubated for 2 h at 37 °C in 20 mM HEPES, pH 7.4, 1 mM $MgCl_2$, and 0.2 mCi/ml [*choline-methyl*-^{14}C]sphingomyelin (Amersham Pharmacia Biotech, United Kingdom; 20,000 Bq per assay). Released radioactive phosphocholine was extracted with chloroform/methanol (2:1, v/v) and quantified by liquid scintillation counting.

RESULTS

PPME Localizes in Membranes and in Lysosomes—Since it has been previously demonstrated that many hydrophobic derivatives of porphyrin localize at the cell membrane (46), we decided to investigate whether PPME exhibited a similar cellular distribution. Incubation of HCT-116 cells in the presence of 2 μM PPME for 17 h allowed us to detect a strong PPME fluorescence at the cytoplasmic membrane and in several internal compartments (Fig. 1*B*). To characterize the nature of the intracellular compartments where PPME accumulated, cells were co-incubated with PPME and various fluorescent probes. Using rhodamine 123 as a fluorescent stain of mitochondria (47), it was evident that no PPME accumulated inside the mitochondria, even after long incubation times, *e.g.* overnight incubation (data not shown). Cells were incubated with 1 μM PPME for 18 h and then with 2 μM neutral red for the last 30 min prior to irradiation. Under this condition, in the absence of a prolonged wash, neutral red was expected to stain mainly the endoplasmic reticulum-Golgi complex (48). Fig. 2*A* demonstrates that, whereas the red fluorescence of PPME could be easily observed, practically no fluorescence was recorded using a green filter that allowed detection of neutral red emission (48). This was further illustrated in Fig. 2*B* with spectrotopographic images. At the onset of irradiation, red fluorescence of PPME at 677 nm was observed without any strong contribution in the 500–550 nm range. Twenty seconds after the beginning of the irradiation, virtually all the PPME fluorescence was bleached, but a significant increase in the green fluorescence

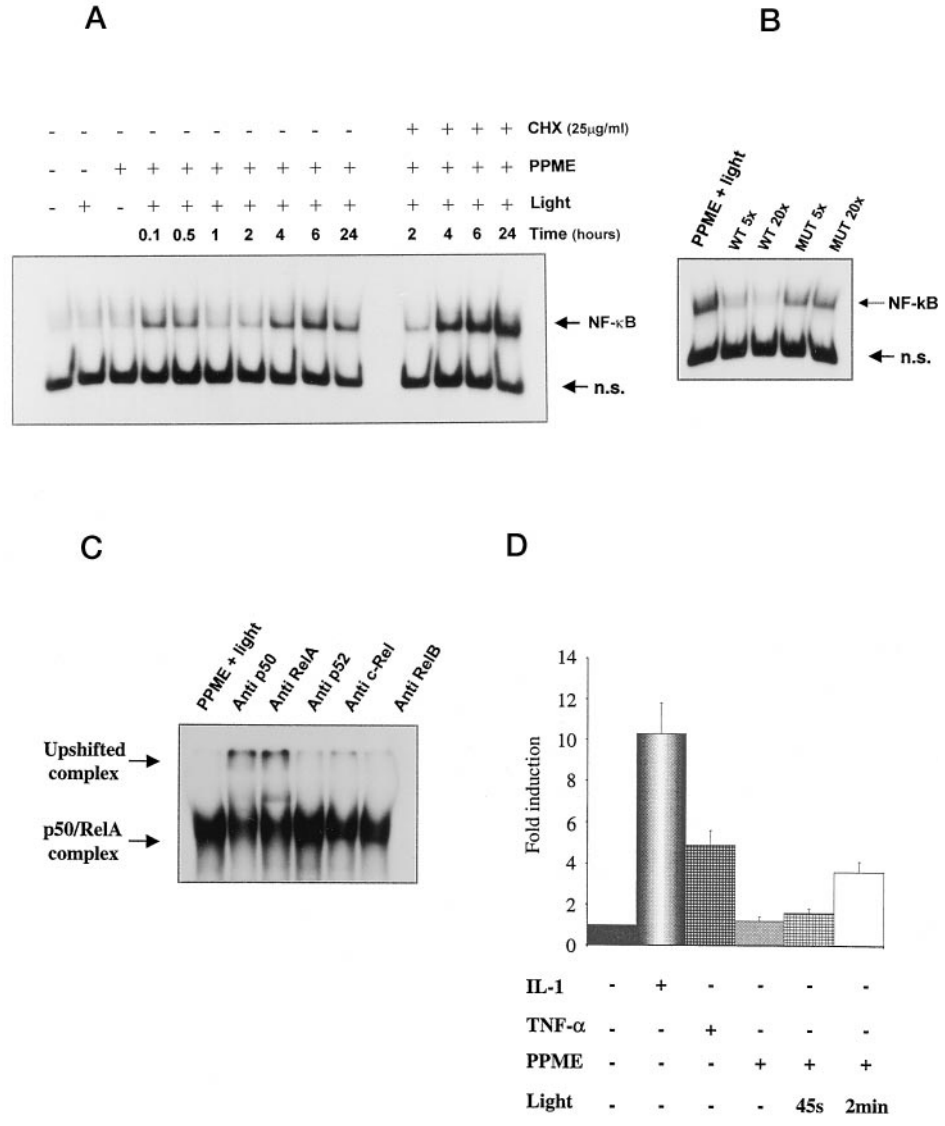

FIG. 3. **The effect of PPME photoreaction on κB-DNA binding activities in HCT-116 cells.** *A,* induction of a nuclear κB enhancer DNA-binding protein after treatment of HCT-116 cells with 2 μM PPME for 17 h and 200 s of irradiation with red light. HCT-116 cells were also preincubated for 60 min in the presence of cycloheximide (*CHX*) at 25 μg/ml. Nuclear extracts were prepared at various times after irradiation, and equal amounts of protein were mixed with a ^{32}P-labeled κB probe. Samples were loaded on 6% native polyacrylamide gels and electrophoresed at 150 V. The autoradiogram of the gel is shown, and the *arrow* indicates the position of the specific complex; the nonspecific DNA binding was noted, *n.s.* (the position of the free probe was not shown). *B,* competition analysis. Nuclear extracts from HCT-116 cells photosensitized with 2 μM PPME were prepared 240 min after the light treatment and analyzed by EMSA as in *A*. Nuclear extracts were either mixed directly with the ^{32}P-labeled probe or with the labeled probe in the presence of 5 or 20 molar excess of wild-type or mutated κB probe. *C,* immunoreactivity of the PPME-inducible protein-κB enhancer complex. Nuclear extracts from HCT-116 cells photosensitized as above were either mixed directly with the ^{32}P-labeled κB probe or incubated with antisera specific for p50, RelA, c-Rel, RelB, and p52 before being mixed with the ^{32}P-labeled κB probe. Samples were then loaded on a 6% polyacrylamide native gel and electrophoresed. *D,* transient transfection assay of HCT-116 cells with a κB-Luc reporter construct. HCT-116 cells were transfected with 0.1 μg of κB-Luc before being treated with 150 units/ml IL-1β or 150 units/ml TNF-α for 24 h or with 2 μM PPME with or without light and then left in culture for 15 h. Luciferase activity was then measured in cell extracts and expressed as fold increase over untreated cells.

with a maximum toward 570 nm was observed. Such a maximum was in agreement with neutral red localization in the endoplasmic reticulum-Golgi complex (48). It was therefore suggested that neutral red as well as some PPME co-localized in this environment, leading to the quenching of neutral fluorescence probably by singlet-singlet energy transfer from neutral red to PPME. Irreversible PPME photobleaching inhibited the energy transfer process and restored neutral red fluorescence. Cells were also incubated with 0.25 μM PPME and 1 μM lucifer yellow for 18 h. Under these conditions and as expected, the lysosomotropic dye lucifer yellow accumulated into lysosomes as shown in Fig. 2*C*. This figure also demonstrated that, in addition to weak uniform fluorescence, spots that perfectly match those obtained with lucifer yellow fluorescence were observed. Moreover, sequences of images obtained with a green filter to isolate the lucifer yellow fluorescence from that of PPME showed a rapid decrease of that fluorescence, thereby suggesting lysosome destabilization since no loss occurred when cells were loaded with lucifer yellow alone (data not shown). In order to confirm whether PPME could localize in the endoplasmic reticulum and/or in the Golgi apparatus, we incubated HCT-116 cells with 0.5 μM PPME during 15 h and then with BCP (4 μM) during 15 min. BCP emits a red fluorescence only in an aggregated form which is promoted in the Golgi apparatus and in the Golgi vesicles, whereas in the monomeric form it binds to internal membranes or to the cytoplasmic membrane where it emits a green fluorescence (49). As shown in Fig. 2*D*, BCP emitted only a green fluorescence due to a

localization in the cytoplasmic membrane and in the endoplasmic reticulum. This probe turned out to perfectly co-localize with PPME (Fig. 2*D*). These data were confirmed by using a carbocyanine derivative (DiOC6) which is a green fluorescent marker of the endoplasmic reticulum (50). As shown in Fig. 2*F*, incubation of HCT-116 cells with PPME as above and addition of DiOC6 (2 mg/ml) during 15 min allowed us to observe a clear co-localization of the two fluorescent molecules in the endoplasmic reticulum. These data unambiguously demonstrate that PPME accumulated at the cytoplasmic membrane but also in lysosomes and in the endoplasmic reticulum.

NF-κB Activation Occurs in Two Separate Waves—Determining whether photodynamic photosensitizers such as PPME which localized in cytoplasmic and in internal membranes could activate NF-κB was of interest because it could lead to important information on a possible immunomodulation by tumor cells treated by such a photoactive drug. To this end, HCT-116 cells were incubated for 17 h in the dark with 2 μM PPME and then irradiated with red light. Nuclear extracts were prepared at various times after photosensitization and analyzed by EMSA. As shown in Fig. 3*A*, an important retarded band appeared transiently after irradiation with its maximal intensity observed between 10 and 30 min. The intensity of the band decreased, almost disappearing after 1 h. A second wave of NF-κB activation could then be observed 2 h after irradiation (Fig. 3*A*). Contrary to the first wave of activation, the second appeared slowly and was sustained up to 24 h. This is the first demonstration that an inducing agent could activate NF-κB in two separate waves as follows: a rapid and transient phase followed by a slower and sustained one. Competition experiments carried out with a wild-type or a mutated unlabeled NF-κB probe demonstrated that the upper retarded band was specific, whereas the lower one was not (Fig. 3*B*). To determine whether the second phase of activation was due to a post-transcriptional mechanism, HCT-116 cells were preincubated with cycloheximide for 60 min before being photosensitized by PPME. As shown in Fig. 3*A*, the intensity of the NF-κB band was not decreased by cycloheximide, demonstrating that the two waves of NF-κB activation were due to a post-transcriptional activation mechanism. Using antibodies directed against the various members of the Rel/NF-κB family (p50, RelA, c-Rel, RelB, and p52), we also observed that the retarded complex involved the classical p50/RelA heterodimer (Fig. 3*C*).

In order to ascertain whether the NF-κB complex induced by PPME and light was transcriptionally active, we transiently transfected HCT-116 cells with a κB-Luc reporter plasmid construct. As shown in Fig. 3*D*, transfected HCT-116 cells incubated with PPME in the dark did not give rise to detectable κB-driven transcriptional activity, whereas photosensitization of the transfected HCT-116 cells allowed us to detect increased transcriptional activity (4-fold), demonstrating that the p50/RelA heterodimer found in cell nuclei by EMSA was transcriptionally active. On the other hand, classical NF-κB inducers such as TNF-α or IL-1β led to a 5- and 10-fold increase in the κB-driven transcriptional activity, respectively (Fig. 3*D*).

Western blot analysis of cytoplasmic extracts from HCT-116 cells photosensitized by PPME also showed a rapid and transient decrease in the amount of the IκBα molecule after 30 min (Fig. 4*A*). Analysis of the band intensity revealed that about 50% of the cytoplasmic IκBα pool was degraded after 30 min. Similarly to what was observed by EMSA (see Fig. 3*A*), the IκBα degradation is transient and the cytoplasmic IκBα pool was replenished after 1 h before starting again to decrease (Fig. 4*A*). Concomitantly to what was observed by EMSA, this second wave of IκBα degradation was slow and sustained. After 24 h almost all the IκBα pool was degraded. These data unambiguously demonstrated that NF-κB activation by PPME and red light involved IκBα degradation in two different waves, likely involving different mechanisms. The fate of three other inhibitory Rel proteins was also followed by Western blots. As shown in Fig. 4, *B–D*, neither IκBβ, p105, nor p100 inhibitors were degraded following PPME photosensitization, showing that in HCT-116 cells most of the NF-κB activation mechanism was controlled by IκBα degradation.

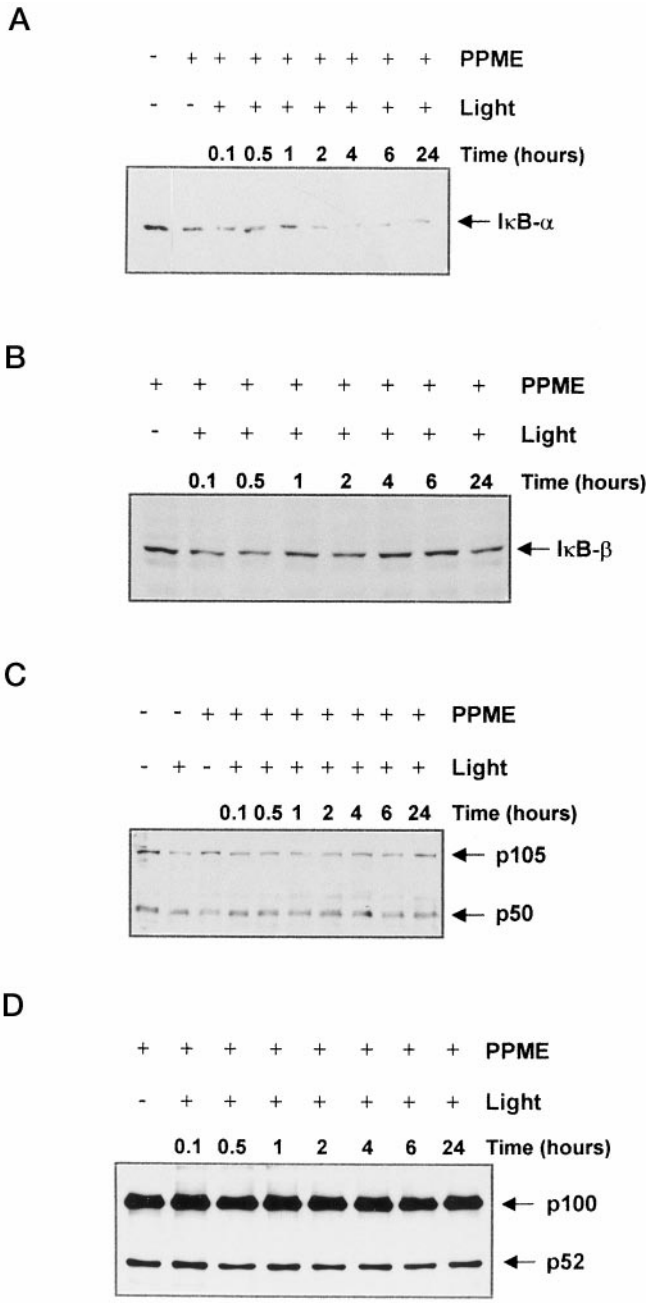

FIG. 4. **Analysis of the NF-κB inhibitory proteins after treatment of HCT-116 cells with PPME and light.** Cytoplasmic extracts were prepared at various times after the photoreaction and analyzed by Western blot with different antibodies. *A,* IκBα; *B,* IκBβ; *C,* p105; and *D,* p100. The *arrows* indicate the position of the various inhibitory proteins.

Singlet oxygen has frequently been involved as secondary messenger in cells treated by photodynamic therapy (9–12). In order to evaluate the role of this reactive oxygen species in NF-κB activation, HCT-116 cells were irradiated in PBS where H_2O was replaced by D_2O, since singlet oxygen lifetime is increased by this isotopic substitution (51). EMSA analysis

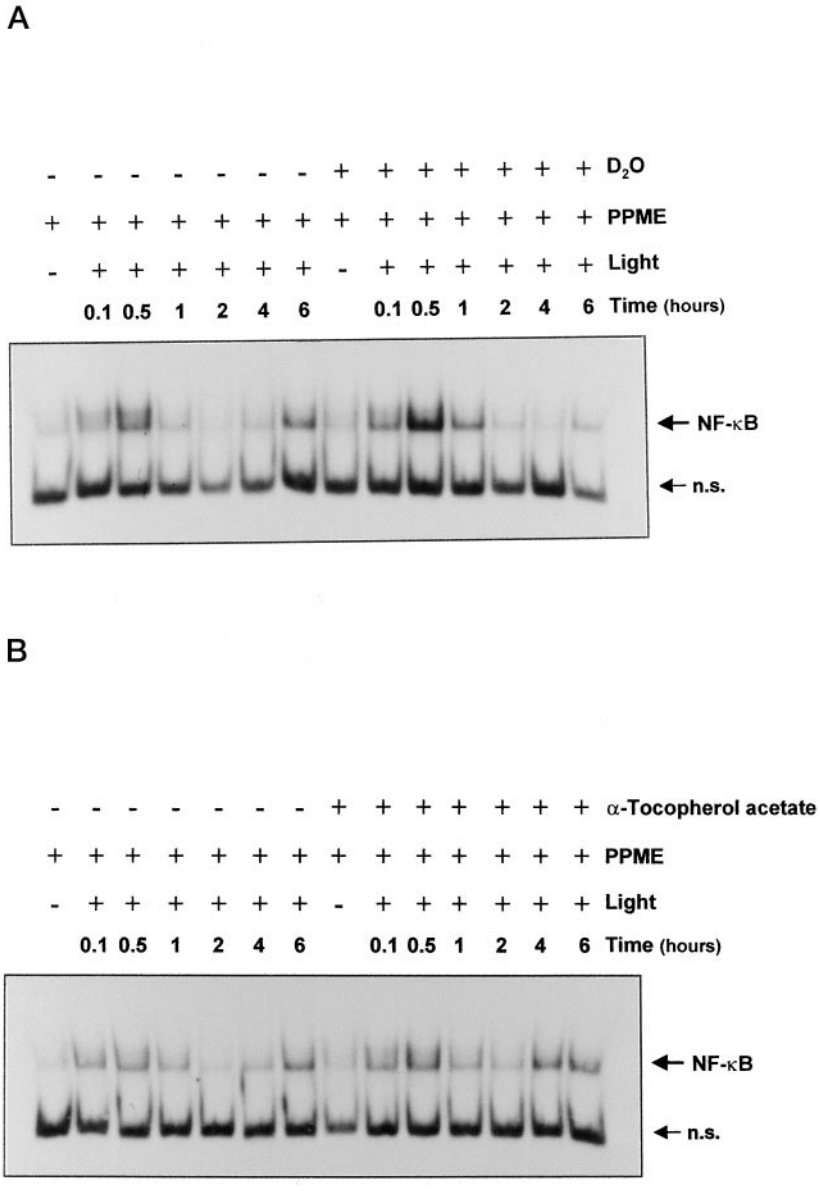

FIG. 5. *A,* EMSA analysis of NF-κB activity in nuclear extracts of HCT-116 cells treated with 2 μM PPME and light in the presence or absence of deuterium oxide. EMSA were carried out as in Fig. 3, and the *arrows* indicate the specific NF-κB complex and a nonspecific band (*n.s.*). *B,* EMSA analysis of NF-κB activity in nuclear extracts of HCT-116 cells treated with 2 μM PPME and light in the presence or absence of α-tocopherol (vitamin E) acetate (400 μM added 24 h before irradiation). EMSA were carried out as in Fig. 3, and the *arrows* indicate the specific NF-κB complex and a nonspecific band (*n.s.*).

revealed that isotopic substitution significantly increased the intensity of the p50-RelA complex found in the nucleus of HCT-116 cells photosensitized by PPME (Fig. 5*A*). Interestingly, this increase in band intensity was mainly detectable during the first rapid and transient phase (Fig. 5*A*). However, these data by themselves could not directly implicate singlet oxygen as a mediator of NF-κB activation because isotopic replacement could modify other physicochemical parameters such as excited state lifetime (51). In order to clarify this point, we decided to investigate the effects of several antioxidant molecules (*e.g.* singlet oxygen quenchers) on NF-κB activation by PPME photosensitization. Many studies have shown that antioxidants blocked NF-κB activation by ROS such as hydrogen peroxide (14) but also when pro-inflammatory cytokines were used as stimuli (15). The chosen antioxidants were as follows: (i) classical hydrophilic molecules such as *N*-acetyl-L-cysteine (40 and 50 mM added 60 min before irradiation), pyrrolidine 9-dithiocarbamate (100–500 μM added 60 min before irradiation), and Trolox (a water-soluble derivative of vitamin E, 500 μM added 90 min before irradiation); and (ii) lipophilic antioxidants such as vitamin E (100 and 400 μM added either 60 min or 24 h before irradiation) and vitamin E acetate (400 μM added 24 h before irradiation). As shown in Fig. 5*B*, vitamin E acetate and all other of these antioxidant molecules did not exhibit inhibitory effects on NF-κB activation in HCT-116 cells by PPME photosensitization indicating that the intracellular release of ROS was probably not involved in NF-κB activation. To determine further whether ROS were involved or not in NF-κB activation by PPME photosensitization, lipoperoxides were measured by TBARs assay. Under experimental conditions leading to maximal NF-κB activation, there was no lipoperoxide detectable in treated HCT-116 cells, confirming that NF-κB activation by PPME photosensitization did not involve ROS generation and membrane peroxidation.

PPME Photosensitization Promotes IL-1 Receptor Internalization—Detection in HCT-116 cells photosensitized by PPME of a rapid and transient activation of NF-κB could mimic what was observed in many cell types after treatment with cytokines. To determine whether PPME photosensitization mimicked cell activation by cytokines, we investigated the effects of PPME photosensitization on cytokine receptor in terms of receptor internalization. We first looked at IL-1 receptor internalization. As shown in Fig. 6*A,* addition of radiolabeled IL-1β to HCT-116 allowed us to observe its internalization within 30 min of incubation at 37 °C (*lanes 1–3*). This internalization could be competed out by preincubation of cells with unlabeled

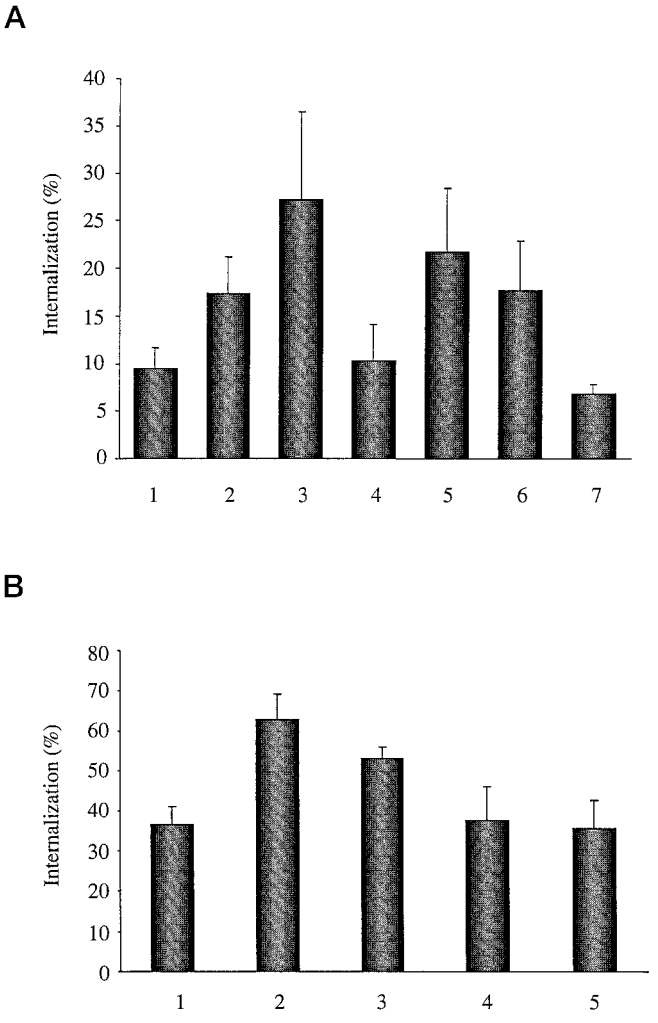

FIG. 6. *A,* PPME promotes IL-1 receptor internalization in HCT-116 cells. HCT-116 cells were incubated for 2 h at 4 °C with radiolabeled IL-1β and then placed for 0 min (*lane 1*), 15 min (*lane 2*), or 30 min (*lane 3*) at 37 °C to allow internalization of the receptor. *Lane 4,* HCT-116 cells were preincubated for 15 min with unlabeled IL-1β before addition of radiolabeled IL-1β and incubated a further 15 min at 37 °C. *Lane 5*, HCT-116 cells were pretreated for 20 h at 37 °C with 2 μM PPME and illuminated before addition of radiolabeled IL-1β. *Lane 6,* HCT-116 cells were pretreated for 15 min at 4 °C with 2 μM PPME and illuminated before addition of radiolabeled IL-1β. *Lane 7* is identical to *lane 6*, except that HCT-116 cells were incubated first with cold IL-1β for 15 min at 4 °C. *B,* PPME does not influence TNF-α receptor internalization. HCT-116 cells were incubated for 2 h at 4 °C with radiolabeled TNF-α before being placed at 37 °C for 0 min (*lane 1*) or 30 min (*lane 2*). *Lane 3*, HCT-116 cells were preincubated with unlabeled TNF-α before being treated as in *lane 2*. *Lane 4*, HCT-116 cells were preincubated for 20 h at 37 °C with 2 μM PPME and illuminated before being incubated in the presence of radiolabeled TNF-α for 2 h at 4 °C. *Lane 5* is identical to *lane 4*, except that preincubation with PPME was carried out at 4 °C for 15 min. Internalization was determined as the ratio between the amount of the radiolabeled cytokine taken up by cells and that remaining outside cells.

IL-1β (Fig. 6*A, lane 4*). When HCT-116 cells were incubated with PPME for 20 h at 37 °C (*lane 5*) or for 15 min at 4 °C (*lane 6*) and then irradiated and pulsed with radiolabeled IL-1β, there was a significant increase in IL-1 receptor internalization (Fig. 6*A*). When cells were treated in a similar manner but preincubated with unlabeled IL-1β before PPME was added to HCT-116 cells, no internalization could be detected (Fig. 6*A, lane 7*), demonstrating that PPME photosensitization promoted IL-1 type I receptor internalization.

Since other cytokine receptors could be involved in the reaction, we measured the effect of PPME photosensitization on TNF receptor. As shown in Fig. 6*B*, addition of radiolabeled TNF-α to HCT-116 cells made it possible to follow TNF receptor internalization within 30 min at 37 °C (*lane 2*). Again, preincubation with unlabeled TNF-α significantly decreased internalization (Fig. 6*B, lane 3*). Conversely to what was observed with IL-1 receptor, PPME photosensitization did not promote TNF receptor internalization (Fig. 6*B, lanes 4* and *5*), demonstrating that its effect was specific to the IL-1 receptor.

IL-1 Signaling Mediates NF-κB Activation by PPME Photosensitization—The demonstration that PPME photosensitization could favor IL-1 receptor internalization yielding a rapid and transient activation of NF-κB prompted us to determine whether PPME photosensitization activates NF-κB through the IL-1 signaling pathway. To investigate this, HCT-116 cells were transfected with a κB-Luc reporter plasmid construct together with various plasmids expressing mutant or wild-type TRAF6 protein, which is associated with the IL-1 receptor (34). HCT-116 cells were then either photosensitized with PPME or treated with IL-1β or TNF-α. As shown in Fig. 7*A,* the expression of TRAF6 in HCT-116 cells prior to stimulation did not significantly modify κB-driven transcriptional activity in cells photosensitized with PPME or treated with IL-1β. In cells treated with TNF-α, TRAF6 overexpression slightly inhibited κB-driven transcriptional activity (Fig. 7*A*). However, when HCT-116 cells were co-transfected with a dominant negative version of TRAF6 (ΔTRAF6), there was a clear down-regulation of NF-κB transactivation in cells treated with IL-1β or photosensitized by PPME, *i.e.* luciferase activities were lower than 50% of the control with 1 μg of ΔTRAF6 (Fig. 7*A*). In the case of HCT-116 treated with TNF-α, co-transfection with ΔTRAF6 led also to a dose-dependent decrease in transcriptional activity, but luciferase activity remained close to the control value at the lowest ΔTRAF6 concentrations (0.1 and 0.25 μg). These data showed that PPME photosensitization and IL-1β stimulation induced similar effects on transcription controlled by a κB gene promoter, whereas TNF-α induced κB-dependent transcription through a distinct pathway.

The role of TRAF2, an adaptor molecule associated with the TNF receptor, was also investigated in the same assay (35). As shown in Fig. 7*B*, expression of a TRAF2 dominant negative protein (ΔTRAF2) decreased κB-driven transcriptional activity in HCT-116 cells treated with TNF-α in a dose-dependent manner, whereas there was no effect on cells photosensitized by PPME or treated by IL-1β. These data were in agreement with the experiments where the receptor internalization was measured and confirmed that PPME photosensitization could not recruit members of the TNF-signaling pathway.

Recently, IκB kinases (IKK-α and -β) have been identified as the main cellular kinases carrying out IκBα phosphorylation on serine residues 32 and 36 after cell induction with pro-inflammatory cytokines (IL-1β and TNF-α) (26–29). In order to verify whether IKKs could be activated by PPME photosensitization, HCT-116 cells were co-transfected by the κB-luciferase reporter plasmid and a plasmid expressing either IKK-α or IKK-β or IKK-α and -β. As shown in Fig. 8*A*, overexpression of IKK-α or -β in unstimulated HCT-116 cells increased κB-driven transcriptional activity. Co-overexpression of IKK-α and -β yielded a synergistic activation giving rise to 11-fold induction of the κB-driven transcription (Fig. 8*A*). Similarly, overexpression of IKK-α or -β or IKK-α plus -β increased in a dose-dependent fashion κB-driven transcriptional activity in HCT-116 cells treated with either TNF-α (Fig. 8*B*) or IL-1β (data not shown). Similarly, when HCT-116 cells were transfected to overexpress IKKs before being photosensitized with PPME, there was a significant increase of the κB-driven transcription; this effect was particularly significant when both IKK-α and -β

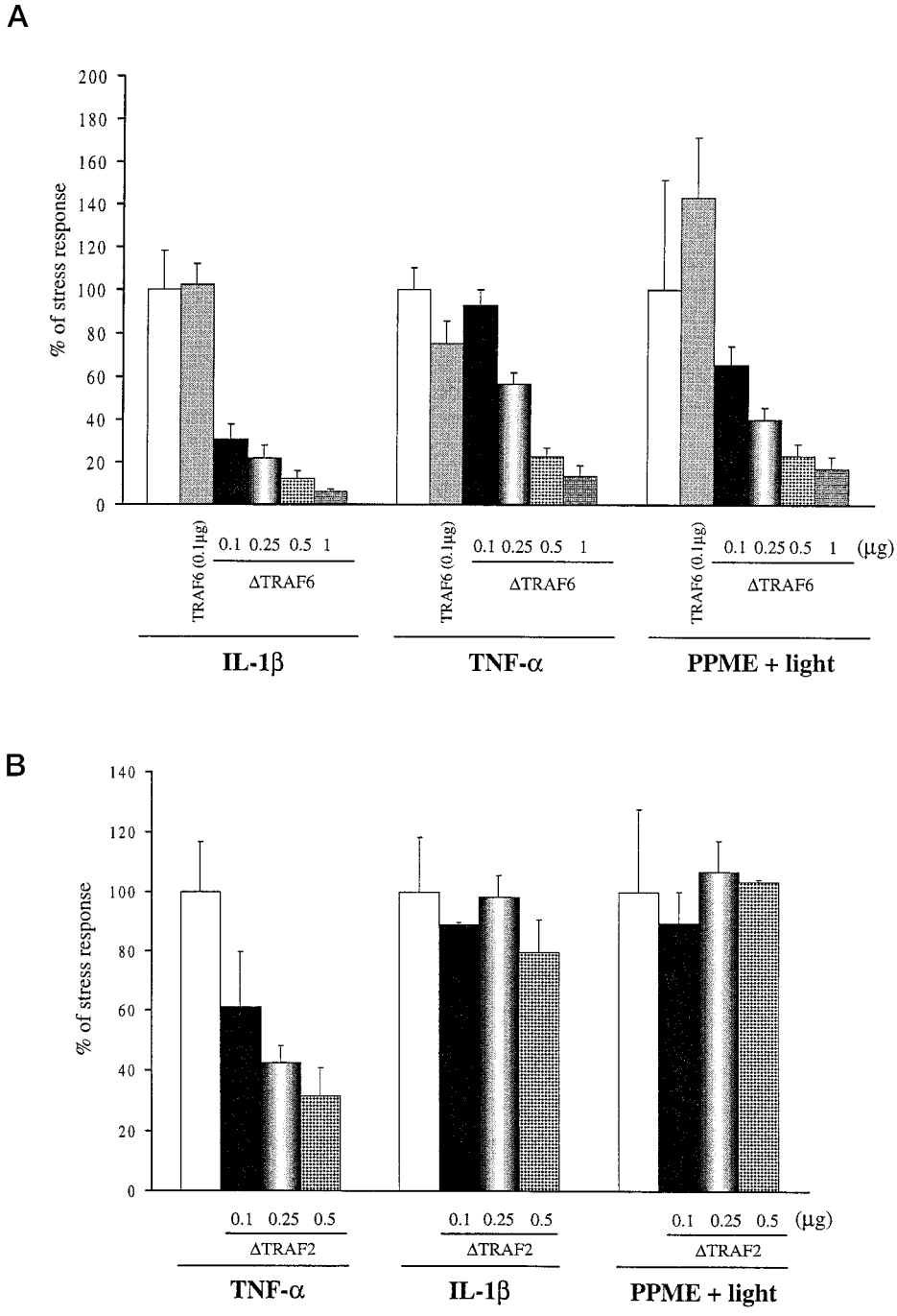

FIG. 7. **HCT-116 cells transient transfection assays with 0.1 μg of κB-Luc reporter plasmid in the presence of plasmids expressing various signaling proteins.** Luciferase activities were measured on cell extracts and expressed as a percentage of the luciferase activity obtained in cells induced either by TNF-α or IL-1β or by PPME photosensitization. *A,* co-transfection was carried out either with 0.1 μg of TRAF6 expression plasmid or with increasing amounts of a plasmid expressing a dominant negative version of TRAF6 (from 0.1 to 1 μg). Cells were treated either with 150 units/ml IL-1β for 24 h or with 150 units/ml TNF-α for 24 h or treated with 2 μM PPME and irradiated for 2 min before being replaced in culture for 15 h. *B,* co-transfection was carried out with either 0.1 μg of TRAF2 expression plasmid or with increasing amounts of a plasmid expressing a dominant negative version of TRAF2 (from 0.1 to 1 μg). Cells were treated either with IL-1β or TNF-α or with PPME and light as in *A.*

were co-expressed (Fig. 8*C*). To confirm the involvement of IKKs in the PPME-mediated NF-κB activation, one HCT-116 cell line overexpressing IκBα mutated at serines 32 and 36 (S32A,S36A) was constructed (MUT4). In addition, an HCT-116 cell line overexpressing IκBα mutated at tyrosine 42 (Y42F) was also generated (Tyr-42). These two cell lines were then photosensitized as described above, and nuclear extracts were prepared after various times to be analyzed by EMSA. As shown in Fig. 8*D*, a classical NF-κB complex can be visualized in wild-type HCT-116 cells and in HCT-116 Tyr-42 cells. On the other hand, in the cell line (MUT4) overexpressing IκBα S32A,S36A, there was no NF-κB complex induced by photosensitization demonstrating again that NF-κB activation by PPME required IKKs and IκBα phosphorylation on serines 32 and 36. These data led to identifying IKKs as the main IκBα kinases stimulated by PPME photosensitization.

NF-κB Activation by PPME Involves Ceramide Generation—Ceramide is a second messenger involved in signaling pathways following TNF-α or IL-1β stimulation (44, 52). Ceramide production after cellular stimulation with pro-inflammatory

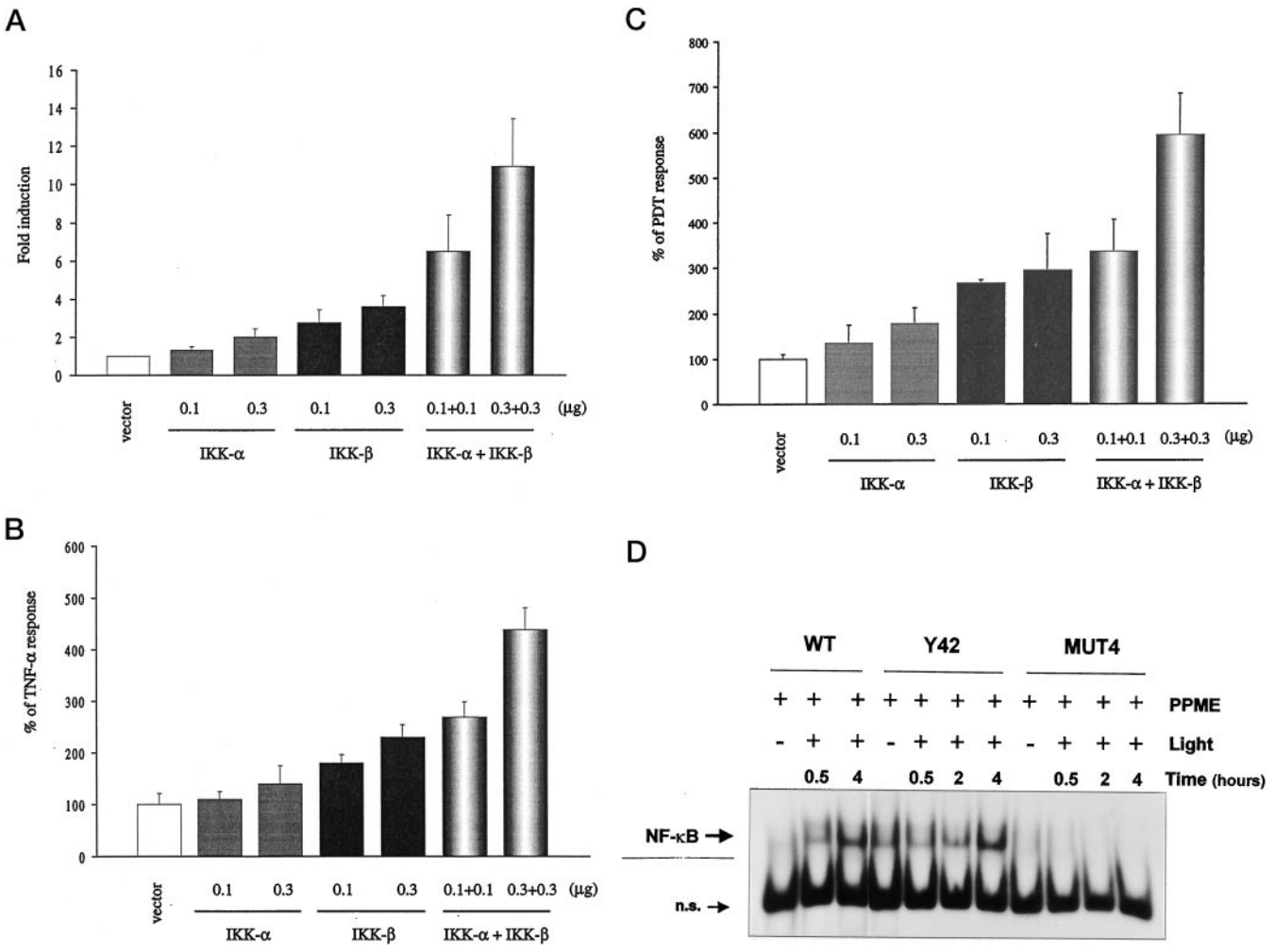

FIG. 8. **HCT-116 cells transient transfection assays with 0.1 μg of κB-Luc reporter plasmid in the presence of plasmids expressing IκBα kinases (IKK-α or -β).** *A,* co-transfection was carried out with increasing amounts of IKK-α or IKK-β or IKK-α plus -β expression plasmids (0.1 and 0.3 μg). Luciferase activities were measured on cell extracts and expressed as fold increase *versus* untransfected cells. *B,* co-transfection was carried out with increasing amounts of IKK-α or IKK-β or IKK-α plus -β expression plasmids (0.1 and 0.3 μg) before being treated with TNF-α (150 units/ml) as in Fig. 7. Luciferase activities were measured on cell extracts and expressed as percentage of the luciferase activity in HCT-116 cells treated with TNF-α alone. *C,* co-transfection was carried out with increasing amounts of IKK-α or IKK-β or IKK-α plus -β expression plasmids (0.1 and 0.3 μg) before being photosensitized with PPME as in Fig. 7. Luciferase activities were measured on cell extracts and expressed as percentage of the luciferase activity in HCT-116 cells photosensitized with PPME alone. *D,* EMSA analysis of NF-κB activity in nuclear extracts of HCT-116 cells (*WT*), of HCT-116 cells overexpressing IκBα mutated at serines 32 and 36 (*MUT4*), and of HCT-116 cells overexpressing IκBα mutated at tyrosine 42 (*Y42*). These cells were grown in similar conditions before being treated with 2 μM PPME and light. EMSA were carried out as in Fig. 3, and the *arrows* indicate the specific NF-κB complex and a nonspecific band (*n.s.*).

cytokines results from sphingomyelin hydrolysis catalyzed by either the acidic or the neutral sphingomyelinase (SMase). It was reported that these two enzymes are linked to distinct pathways following interaction of TNF-α with TNF receptor 1 (53) or IL-1β to its type 1 receptor (52). Since PPME photosensitization utilized IL-1 signaling proteins to activate NF-κB, ceramide production was measured at various times after photosensitization. As shown in Fig. 9*A,* total ceramide significantly increased as early as 10 and 30 min after photosensitization, reaching its maximal value after 2 h before gradually declining at longer times. A similar behavior was recorded in HCT-116 cells treated with TNF-α (Fig. 9*A*). These data demonstrated that ceramide generation occurred soon after photosensitization but remained elevated for at least 6 hours, indicating that ceramide could be considered as being a messenger of the second wave of NF-κB induction by PPME photosensitization.

Since ceramide release could be attributed to either acidic or neutral SMase activation, these two enzymatic activities were determined in HCT-116 cells treated with TNF-α or photosensitized by PPME. From the data presented in Fig. 9*B*, it is evident that both TNF-α and PPME photosensitization led to acidic SMase activation. This activation was transient and appeared somewhat earlier than the release of ceramide. On the other hand, neutral SMase activity was measured on extracts from HCT-116 cells treated with 150 units/ml TNF-α or photosensitized with PPME. Although the basal activity of neutral SMase was rather low in HCT-116 cells, it was increased 1.3-fold after 15 min of treatment with TNF-α (data not shown). However, no neutral SMase activation could be detected after PPME photosensitization (data not shown), demonstrating that ceramide generation following photosensitization was totally due to acidic SMase activation.

To demonstrate further the involvement of acidic SMase and ceramide in NF-κB activation by PPME photosensitization, two experiments were carried out. First, chloroquine (100 μM), an acidic SMase inhibitor, was added 60 min prior to HCT-116 cell photosensitization with PPME, and NF-κB activation was evaluated by EMSA both 30 min and 24 h after photosensitization. As shown in Fig. 10*A,* chloroquine addition significantly de-

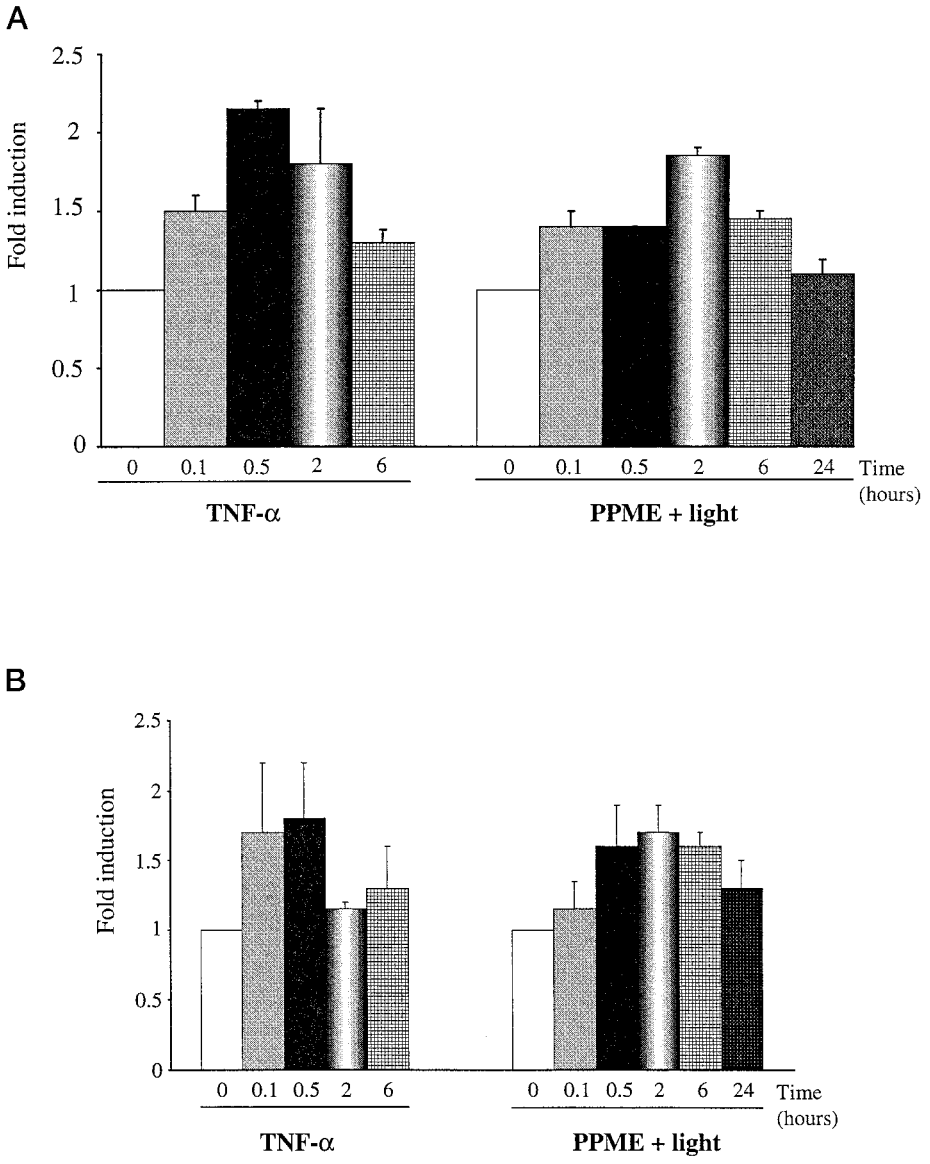

FIG. 9. *A,* ceramide production in HCT-116 cells treated either with 150 units/ml TNF-α or with PPME and light. HCT-116 cells were labeled with 2 μCi/ml 9,10-[^{3}H]palmitic acid. After 24 h labeling, the medium was removed; the cells were stimulated for the indicated times, and total cellular ceramide was determined. Values are indicated as fold stimulation of the control (unstimulated cells). *B,* activation of the acidic sphingomyelinase activity in HCT-116 cells treated either with 150 units/ml TNF-α or PPME and light. Values are indicated as fold induction of the control (unstimulated cells).

creased NF-κB activation during the first (30 min) and second activation wave (24 h), showing that acidic SMase could be considered as a mediator of the response to PPME photosensitization. Second, C_2-ceramide was also added to HCT-116 cells to mimic their release by the activation of acidic SMase. As shown in Fig. 10*B*, NF-κB activation could be clearly visualized by addition of C_2-ceramide on HCT-116 cells. NF-κB activation was clearly observed both at a short and long time after stress, emphasizing the role of ceramide as second messenger in PPME photosensitization.

DISCUSSION

In this paper, we have shown that pyropheophorbide-a methyl ester, a second generation photosensitizer, is a strong activator of the NF-κB transcription factor. The underlying mechanism is rather uncommon; PPME localizes in membranes and promotes IL-1 receptor internalization upon photosensitization, triggering the transduction machinery linked to the IL-1 receptor. This NF-κB activation is transient and does not require oxidative stress. After 2 h, a second wave of NF-κB action gradually appeared lasting up to 24 h. During these two phases, ceramides were generated, suggesting that these lipids act as second messengers to activate NF-κB at longer times. We postulate that PPME located in the lysosomal membrane is responsible for ceramide generation, since acidic SMase, a lysosomal enzyme, is activated by the photosensitizing action of PPME.

Investigating how pyropheophorbide-a can modulate gene expression is of great importance, because tumor eradication by PDT will likely depend not only on an efficient tumor cell killing but also on the adaptation of tumor cells surviving treatment. Since many important genes involved in the control of the immune system and in the inflammatory reaction are controlled by NF-κB, we have decided to pay attention to the mechanisms by which PPME photosensitization activates NF-κB. Photosensitization has already been shown to induce NF-κB in T lymphocytes (41, 54) and in other cell types (55). Although the mechanisms have not yet been clarified, oxidative stress mediated by photosensitization is likely implicated since antioxidants inhibit NF-κB activation or cellular oxidation products can be detected. $^1O_2$ is known to be the main ROS produced by photosensitization (56) and is proposed by several authors (57–59) as a second messenger in gene activation in human skin fibroblasts irradiated by UV-A. Because its lifetime can be significantly increased by deuterium substitution, the observation that NF-κB translocation is greater in a medium where H_2O is substituted by D_2O suggests that $^1O_2$ could

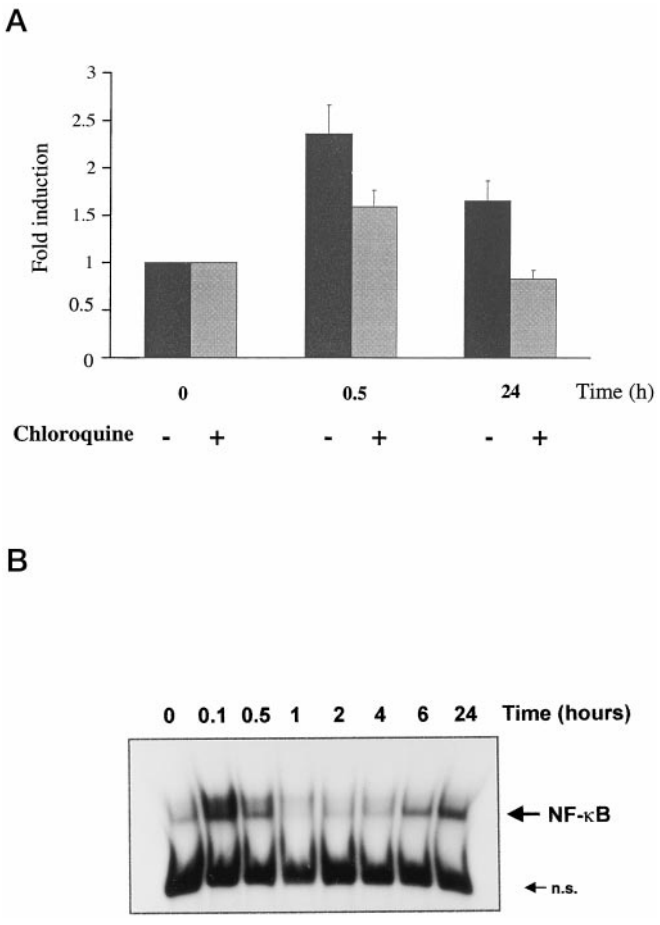

FIG. 10. *A,* effect of chloroquine (100 μM) on NF-κB activation in HCT-116 cells photosensitized by PPME. Chloroquine was added to the cells 60 min prior to PPME photosensitization (carried out as in Fig. 2), and nuclear extracts were prepared after 30 min or 24 h. NF-κB induction was measured by EMSA and expressed in fold induction compared with the control (non-photosensitized cells). The intensities of the specific band were measured by phosphorimaging. *B,* C_2-ceramide induces NF-κB in HCT-116 cells. Cells were treated with 30 μM C_2-ceramide, and nuclear extracts were analyzed by EMSA after various times (from 0 to 24 h). The specificity of the complex was determined by competition with a 50-fold excess of unlabeled wild-type or mutated probe (data not shown).

be involved in the activation mechanism. However, the role of $^1O_2$ as mediator in NF-κB activation by PPME photosensitization could be considered unlikely because (i) none of the tested antioxidants (hydrophilic and hydrophobic) capable of quenching $^1O_2$ inhibit NF-κB activation and (ii) no lipoperoxide can be detected in photosensitized HCT-116 cells. The increased NF-κB activation by PPME photosensitization after D_2O substitution could then be explained by an increased lifetime of the PPME excited state which has already been observed for other photosensitizers (51). This would involve a radical mechanism implicating either an electron or a charge transfer between a PPME excited state and membrane proteins such as the IL-1 type 1 receptor or the acidic SMase. Although a so-called type I reaction would be implicated to explain NF-κB action by PPME photosensitization, we cannot totally rule out that part of the photochemical mechanism could be due to $^1O_2$. Indeed, the lack of inhibition by a lipophilic antioxidant such as vitamin E could also be explained by a subcellular concentration too low to efficiently compete with the reaction between the PPME excited state and membrane receptor. Definitive proof of $^1O_2$ involvement in NF-κB activation could only come from directly measuring its emission at 1268 nm. However, $^1O_2$ detection by infrared emission on cells is currently not feasible.

One of the main contributions of this work is to unambiguously show that PPME photosensitization can specifically mobilize the IL-1 transduction pathway leading to NF-κB activation. This is demonstrated by (i) significant internalization of the IL-1 receptor after photosensitization with PPME; (ii) the inhibition of NF-κB activation by expression of TRAF6 dominant negative, a protein linked to the IL-1 receptor; (iii) the absence of down-regulation by expression of TRAF2 dominant negative mutant protein; and (iv) the increased NF-κB activity when IKK-α, IKK-β, and IKK-α plus -β are overexpressed in photosensitized cells. The type of IL-1 receptor whose internalization is increased by PPME photosensitization is likely to be the type I receptor because the IL-1 type II receptor is not capable of transducing signals and mainly acts as a decoy receptor (60). Interestingly, such an internalization cannot be recorded with the TNF receptor. One explanation could be that PPME cannot promote TNF receptor trimerization, which is required to both transduce signals and promote internalization (61). Whereas the molecular mechanism by which PPME promotes IL-1 receptor internalization is unknown, it could be interesting to determine whether this effect is restricted to receptors that do not require homo- or heterodimerization for their functioning. A modification of cell-surface receptor by PPME photosensitization has recently been published (62); curiously, these authors reported that a mixture between pheorbide-a and PPME can reduce binding of cytokines to their receptors (TNF-α, IL-8, complement factor 5a, and epidermal growth factor). As these data were obtained (i) by measuring cytokine binding to their receptor on neutrophils and (ii) with a mixture of photosensitizers, they reinforce the idea that these compounds can interact with cell-surface receptors and either inactivate them or trigger transduction pathways. The localization of photosensitizers into cellular membranes is therefore expected to be an important determinant controlling the susceptibility of surface proteins. For example, di-hematoporphyrin ether was reported to affect the binding of antibodies to high affinity Fc receptors but not to other surface molecules (63), and methyl pheophorbide-b inhibited the binding of several cytokines to their receptor but not the binding of TNF-α (64). Collectively, these data support the hypothesis that a particular membrane environment, as well as the nature of the receptors, may determine whether the receptor function is activated or inhibited and, therefore, the extent of cell response to PDT.

This new concept is important because it will greatly influence our understanding of the cellular response to PDT not only in terms of tumor cell survival but also of the modification of tumor environment by the release of mediators. As PDT not only reduces tumor burden but also induces inflammation, it is proposed that recruitment of activated macrophages to the inflamed tumor is an important factor in complete tumor eradication (65). In this respect, study of the mechanism of NF-κB activation by PDT is important because many genes encoding cytokines and chemokines are controlled by this factor. Work is now in progress in our laboratory to determine the nature of the genes that are up- and down-regulated by PPME photosensitization. An answer to these questions will lead to a better understanding of the role of host cell response in the antitumor effect of PDT and how the immune response can potentiate antitumor immunity. Recently, it has been demonstrated in a BALB/c mouse model that PDT delivered to normal and tumor tissue *in vivo* causes marked changes in the expression of IL-6 and IL-10 but not of TNF-α, suggesting that the general inflammatory response to PDT may be mediated by IL-6 (66). Because cytokine genes are controlled by NF-κB and by other transcription factors such as AP-1, c-EBP, CREB, etc., the

differential regulation of cytokine genes by PDT could be due to the better inducibility of several transcription factors as opposed to others which could be weakly or not at all regulated by PDT. For example, Photofrin has been shown to lead to a strong and prolonged activation of c-Jun and c-Fos (67), demonstrating that genes having both NF-κB-and AP-1-responsive elements in their promoter are prone to be up-regulated by PDT.

This paper has shown that NF-κB can be considered as a main transcription factor activated by PDT. Mechanism of PPME-mediated NF-κB activation is rather unique because it resembles the response elicited by IL-1 but differs from the response initiated by ROS generation. Membrane localization of PPME is responsible for this peculiar response; the effect on IL-1 receptor and the rapid NF-κB activation is due to PPME in the cytoplasmic membrane, but the slow and sustained NF-κB activation is likely explained by lysosomal PPME localization giving rise to the production of ceramide by activation of the acidic SMase. As many hydrophobic photosensitizers can target the lysosomal membrane (36), it could be postulated that ceramide production could constitute a general response to PDT. Recently, ceramide has been shown to be involved in the PDT-mediated apoptosis of mouse lymphoma cells (68), demonstrating the importance of lipid second messengers both in gene activation and in apoptosis. Since NF-κB has recently been shown to be involved in the control of apoptosis induced by cytokines (68–71) and DNA-damaging drugs (72, 73), the data reported in this paper will add to the understanding of how PPME promotes apoptosis in tumor cells.

Acknowledgment—We thank A-C. Helin for the MUT4 cell line.

REFERENCES

1. Dougherty, T. J. (1993) *Photochem. Photobiol.* **58,** 895–900
2. Pass, H. I. (1993) *J. Natl. Cancer Inst.* **85,** 443–456
3. Fisher, A. M. R., Murphree, A. L., and Gomer, C. L. (1996) *Lasers Surg. Med.* **17,** 2–32
4. Henderson, B. W., and Dougherty, T. J. (1992) *Photochem. Photobiol.* **55,** 145–157
5. Henderson, B. W., Bellnier, D. A., Greco, W. R., Sharma, A., Pandey, R. K., Vaughan, L. A., Weishaupt, K. R., and Dougherty, T. J. (1997) *Cancer Res.* **57,** 4000–4007
6. Bellnier, D. A., Henderson, B. A., Pandey, R. K., Potter, W. R., and Dougherty, T. J. (1993) *J. Photochem. Photobiol. B. Biol.* **20,** 55–61
7. Payne, J. T., Mc Caw, D. L., Casteel, S. W., Frazier, D., Rogers, K., and Tompson, R. V. (1996) *Lasers Surg. Med.* **18,** 406–409
8. Pandey, R. K., Sumlin, A. B., Constantine, S., Aoudia, M., Potter, W. R., Bellnier, D. A., Henderson, B. W., Rodgers, M. A., Smith, K. M., and Dougherty, T. J. (1996) *Photochem. Photobiol.* **64,** 194–204
9. Weishaupt, K. R., Gomer, C. J., and Dougherty, T. J. (1976) *Cancer Res.* **36,** 2326–2329
10. Ito, T. (1978) *Photochem. Photobiol.* **28,** 493–508
11. Athar, M., Muktar, H., and Bickers, D. (1988) *J. Invest. Dermatol.* **90,** 652–657
12. Valenzueno, D. P. (1987) *Photochem. Photobiol.* **46,** 147–160
13. Henderson, B. W., and Dougherty, T. J. (1992) *Photochem. Photobiol.* **55,** 145–157
14. Daziano, J. P., Steenken, S., Chabannon, C., Mannoni, P., Chanon, M., and Julliard, M. (1996) *Photochem. Photobiol.* **64,** 712–719
15. Schreck, R., Rieber, P., and Baeuerle, P. A. (1991) *EMBO J.* **10,** 2247–2258
16. Schreck, R., Meier, B., Mannel, D. N., Dröge, W., and Baeuerle, P. A. (1992) *J. Exp. Med.* **175,** 1181–1194
17. Siebenlist, U., Franzoso, G., and Brown, K. (1994) *Annu. Rev. Cell Biol.* **10,** 405–455
18. Baeuerle, P. A., and Henkel, T. (1994) *Annu. Rev. Immunol.* **12,** 141–179
19. Miyamoto, S., and Verma, I. M. (1995) *Adv. Cancer Res.* **66,** 255–292
20. Beg, A. A., and Baldwin, A. S. (1993) *Genes Dev.* **7,** 2064–2070
21. Haskill, S., Beg, A. A., Tompkins, S. M., Morris, J. S., Yurochko, A. D., Sampson- Johannes, A., Mondal, K., Ralph, P., and Baldwin, A. S., Jr. (1991) *Cell* **65,** 1281–1289
22. Mercurio, F., DiDonato, J. A., Rosette, C., and Karin, M. (1993) *Genes Dev.* **7,** 705–718
23. Rice, N. R., MacKichan, M. L., and Israël, A. (1992) *Cell* **71,** 243–253
24. Brown, K., Park, S., Kanno, T., Franzoso, G., and Siebenlist, U. (1993) *Proc. Natl. Acad. Sci. U. S. A.* **90,** 2532–2536
25. Traenckner, E. B.-M., Pahl, H. L., Henkel, T., Schmidt, K. N., Wilk, S., and Baeuerle, P. A. (1995) *EMBO J.* **14,** 2876–2883
26. Régnier, C. H., Song, H. Y., Gao, X., Goeddel, D. V., Cao, Z., and Rothe, M. (1997) *Cell* **90,** 373–383
27. Song, H. Y., Régnier, C., Kirschning, C. J., Goeddel, D. V., and Rothe, M. (1997) *Proc. Natl. Acad. Sci. U. S. A.* **94,** 9792–9796
28. DiDonato, J. A., Hayakawa, M., Rothwarf, D. M., Zandi, E., and Karin, M. (1997) *Nature* **388,** 548–554
29. Mercurio, F., Zhu, H., Murray, B. W., Shevchenko, A., Bennett, B. L., Li, J. W., Young, D. B., Barbosa, M., and Mann, B. (1997) *Science* **278,** 860–866
30. Yamaoka, S., Courtois, G., Bessia, C., Whiteside, S. T., Weill, R., Agou, F., Kirk, H. E., Kay, R. J., and Israel, A. (1998) *Cell* **93,** 1231–1240
31. Rothwarf, D. M., Zandi, E., Natoli, G., and Karin, M. (1998) *Nature* **395,** 297–300
32. Satriano, J. A., Shuldiner, M., Hora, K., Xing, Y., Shan, Z., and Schlondorff, D. (1995) *J. Clin. Invest.* **92,** 1564–1571
33. Feng, L., Xia, Y., Garcia, G. E., Hwang, D., and Wilson, C. B. (1995) *J. Clin. Invest.* **95,** 1669–1675
34. Cao, Z., Xiong, J., Takeuchi, M., Kurama, T., and Goeddel, D. V. (1996) *Nature* **383,** 443–446
35. Rothe, M., Sarma, V., Dixit, V. M., and Goeddel, D. V. (1995) *Science* **269,** 1424–1427
36. Geze, M., Morliere, P., Maziere, J. C., Smith, K. M., and Santus, R. (1993) *J. Photochem. Photobiol. B. Biol.* **20,** 23–35
37. Gaullier, J. M., Geze, M., Santus, R., Sa E Melo, T., Maziere, J. C., Bazin, M., Morliere, P., and Dubertret, L. (1995) *Photochem. Photobiol.* **62,** 114–122
38. Dignam, D., Lebovitz, R. M., and Roeder, R. G. (1983) *Nucleic Acids Res.* **11,** 1475–1489
39. Andrews, N. C., and Faller, D. V. (1991) *Nucleic Acids Res.* **19,** 2499
40. Franzoso, G., Bours, V., Park, S., Tomita-Yamagushi, M., Kelly, K., and Siebenlist, U. (1992) *Nature* **359,** 207–210
41. Legrand-Poels, S., Bours, V., Piret, B., Pflaum, M., Epe, B., Rentier, B., and Piette, J. (1995) *J. Biol. Chem.* **270,** 6925–6934
42. Solari, R., Smithers, N., Kennard, W., Ray, K., and Grenfell, S. (1994) *Biochem. Pharmacol.* **47,** 93–101
43. Levade, T., Tempesta, M.-C., and Salvayre, R. (1993) *FEBS Lett.* **329,** 306–310
44. Wiegmann, K., Schü tze, S., Machleidt, T., Witte, D., and Kronke, M. (1994) *Cell* **78,** 1005–1015
45. Jaffrézou, J. P., Levade, T., Bettaïeb, A., Andrieu, N., Bezombes, C., Maestre, N., Vermeersch, S., Rousse, A., and Laurent, G. (1996) *EMBO J.* **15,** 2417–2424
46. Kessel, D. (1984) *Biochem. Pharmacol.* **33,** 1389–1393
47. Kim, M., Cooper, D. D., Hayes, S. F., and Spangrude, G. J. (1998) *Blood* **91,** 4106–4117
48. Sousa, C., Sa E Melo, T., Geze, M., Gaullier, J. M., Maziere, J. C., and Santus, R. (1996) *Photochem. Photobiol.* **63,** 601–607
49. Pagano, R. E., Martin, O. C., Kang, H. C., and Haugland, R. P. (1991) *J. Cell Biol.* **113,** 1267–1279
50. Morlière, P., Mzaière, J. C., Santus, R., Smith, C. D., Prinsep, M. R., Stobbe, C. C., Fenning, M. C., Golberg, J. L., and Chapman, J. P. (1998) *Cancer Res.* **58,** 3571–3578
51. Seret, A., Hoebeke, M., and Van de Vorst, A. (1990) *Photochem. Photobiol.* **52,** 601–604
52. Bonizzi, G., Piette, J., Merville, M. P., and Bours, V. (1997) *J. Immunol.* **159,** 5264–5272
53. Belka, C., Wiegeman, K., Adam, D., Holland, R., Neuloh, M., Herrmann, F., Kronke, M., and Brach, M. A. (1995) *EMBO J.* **14,** 1156–1165
54. Piret, B., Legrand-Poels, S., Sappey, C., and Piette, J. (1995) *Eur. J. Biochem.* **228,** 447–455
55. Ryter, S. W., and Gomer, C. J. (1993) *Photochem. Photobiol.* **58,** 753–756
56. Piette, J., Merville, M. P., and Decuyper, J. (1986) *Photochem. Photobiol.* **44,** 793–802
57. Tyrrell, R. M., and Pidoux, M. (1988) *Photochem. Photobiol.* **49,** 407–412
58. Vile, G. F., and Tyrrell, R. M. (1995) *Free Radical Biol. & Med.* **18,** 721–730
59. Grether-Beck, S., Olaizola-Horn, S., Schmidt, H., Grewe, M., Jahnke, A., Johnson, J. P., Bribiva, K., Sies, H., and Krutman, J. (1996) *Proc. Natl. Acad. Sci. U. S. A.* **93,** 14586–14591
60. Martin, U., and Falk, W. (1997) *Eur. Cytokine Netw.* **8,** 5–17
61. Vandevoorde, V., Haegeman, G., and Fiers, W. (1997) *J. Cell Biol.* **137,** 1627–1638
62. Glinski, J. A., David, E., Warren, T. C., Hansen, G., Leonard, S. F., Pitner, P., Pav, S., Arvigo, R., Balick, M. J., Panti, E., and Grob, P. (1995) *Photochem. Photobiol.* **62,** 144–150
63. Krutmann, J. M., Athar, M., Mendel, D. B., Kahn, I. U., Guyre, P. M., Mukhtar, H., and Elmets, C. A. (1989) *J. Biol. Chem.* **264,** 11407–11413
64. Rieman, D. J., Anzano, M. A., Chan, G. W., Imburgia, T. J., Chan, J. A., Jonhson, R. K., and Greig, R. G. (1992) *Oncol. Res.* **4,** 193–200
65. Korbelik, M., Naraparaju, V. R., and Yamamoto, N. (1997) *Br. J. Cancer* **75,** 202–207
66. Gollnick, S. O., Liu, X., Owczarczak, B., Musser, D. A., and Henderson, B. W. (1997) *Cancer Res.* **57,** 3904–3909
67. Kik, G., Messer, G., Plewig, G., Kind, P., and Goetz, A. E. (1996) *Br. J. Cancer* **74,** 30–36
68. Separovic, D., He, J., and Oleinick, N. L. (1997) *Cancer Res.* **57,** 1717–1721
69. Baichwal, V. R., and Baeuerle, P. A. (1997) *Curr. Biol.* **7,** R94–R96
70. Jimi, E., Nakamura, I., Ikeba, T., Akiyama, S., Takahashi, N., and Suda, T. (1998) *J. Biol. Chem.* **273,** 8799–8805
71. Delic, J., Mashedors, P., Omuci, S., Cosset, J. M., Dumont, J., Binet, J. L., and Magdalenat, H. (1998) *Br. J. Cancer* **77,** 1103–1107
72. Jung, M., Zhang, Y., Dimtchev, A., Dritschilo, A. (1998) *Radiat. Res.* **149,** 596–601
73. Kasibhatla, S., Brunner, T., Genestier, L., Echeverri, F., Mahboubi, A., and Green, D. R. (1998) *Mol. Cell* **1,** 543–551

Pyropheophorbide-a Methyl Ester-mediated Photosensitization Activates Transcription Factor NF- κB through the Interleukin-1 Receptor-dependent Signaling Pathway

Jean-Yves Matroule, Giuzeppina Bonizzi, Patrice Morlière, Nicole Paillous, René Santus, Vincent Bours and Jacques Piette

J. Biol. Chem. 1999, 274:2988-3000.
doi: 10.1074/jbc.274.5.2988